Limits on Drawability of Semicrystalline Flexible Polymers

Yves Termonia

Central Research and Development, Experimental Station, E. I. du Pont de Nemours, Inc., Wilmington, Delaware 19880-0356

Received November 6, 1995; Revised Manuscript Received February 29, 1996[⊗]

ABSTRACT: We present a model study of the factors controlling the drawability of semicrystalline flexible polymers. Our approach focuses on the relative importance of the strength, σ_h, of the attractive bonds between chains in the amorphous phase and of that, σ_a, of the same chains free of attraction forces. We find that drawability reaches its maximum value when the ratio of the two strengths falls below a critical value $\sigma_h/\sigma_a \simeq 150$. The maximum draw value itself is controlled by the crystallinity and by the entanglement density in the amorphous phase.

1. Introduction

Uniaxial drawing constitutes the most widely used technique for the production of high-performance materials from flexible-chain polymers.[1,2] The modulus and tensile strength of these materials indeed have been found to increase steadily with the extent of drawing.[3−5] Theoretical studies have also indicated that the polymer molecular weight sets an upper limit to the maximum achievable draw ratio.[3,4,6−8] Under normal conditions, that limit is difficult to achieve experimentally because of the presence of entanglements between chains.[9] These constraints can however be easily removed through solution processing,[10] commonly referred to as gel spinning, which has allowed to reach draw ratios close to the molecular weight limited values.

Recently, it has been recognized that the polarity of the polymer chains also plays a decisive role in controlling drawability.[11] Thus, a recent gel spinning of high molecular weight polyamides has failed to increase their maximum draw ratio beyond the "natural" value $\lambda = 4-5$.[12] That poor drawability has been attributed to the presence of strong hydrogen bonds between neighboring amide groups. It is the purpose of the present work to investigate in detail, from a theoretical point of view, the role of molecular attraction forces on the drawability of polymeric materials. That study is of great importance in view of the renewed interest in flexible hydrogen-bonded polymers, such as nylon, due to their high toughness and flex-fatigue resistance.

2. Model

Our model for the tensile deformation of flexible polymer networks has been described at length in refs 5, 7, 8, and 13. Its essential features and basic assumptions are briefly recapitulated here. In our approach, the *undeformed* (semi)crystalline polymer solid is represented by a two-dimensional network of entanglements connected by chains in a random coil configuration; see Figure 1. Since our model is on the scale of an entanglement length, the individual molecular attraction forces along and between chains are conveniently represented by "overall" elastic bonds further connecting every entanglement to its neighbors.

Our model results of refs 5, 7, 8, and 13 were limited to the case of polyethylene chains for which the attractive forces (VdW bonds) between chains are weak and deformation is entirely controlled by the molecular weight and the entanglement density. For that particular case, the initial crystallites need not be considered as the latter are rather flexible and easily deform at the high temperatures commonly used in drawing. In the present work, details of the initial crystallites are explicitly taken into account. For simplicity, we assume that the latter are of a size comparable to the entanglement length; see Figure 1. A detailed study of the importance of crystallite size can be found in ref 14.

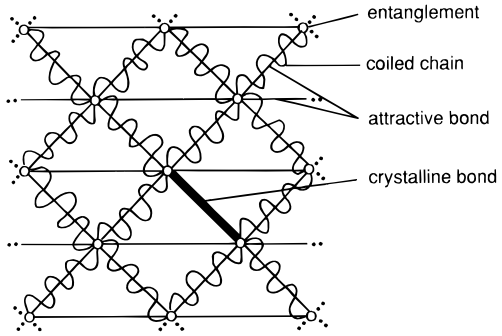

Figure 1. Two-dimensional model representation of an undeformed (semi)crystalline polymer solid. Prior to deformation, all the chain strands between entanglements are in a random coil configuration. The individual molecular attraction forces along chains are conveniently represented by "overall" elastic bonds further connecting every entanglement to its neighbors.

The macromolecular network of Figure 1 is deformed at a constant temperature, T, and rate of deformation, $\dot{\epsilon}$. As the strain on the network increases, an attractive or crystalline bond, i, breaks at a thermally activated rate.[15]

$$\nu_i = \tau \exp[-(U - \beta\sigma_i)/kT] \tag{1}$$

In eq 1, τ is the thermal vibration frequency, U and β are, respectively, the activation energy and volume, and

$$\sigma_i = E\epsilon_i \tag{2}$$

is the local stress. Here, ϵ_i is the local strain and E is the elastic constant ($E = E_h$ for an attractive bond; $E = E_c$ for a crystalline bond). When an attractive bond between two entanglements breaks, our process allows for the underlying chain strand to orient and extend. As in previous work,[16] the stress on an "amorphous" chain strand i is estimated from

$$\sigma_i = E_a n^{1/2}(1/3)L^{-1}(\lambda_i/n^{1/2}) - \sigma_0 \tag{3}$$

where E_a denotes the local modulus at small strains, n

[⊗] Abstract published in *Advance ACS Abstracts,* May 15, 1996.

S0024-9297(95)01661-5 CCC: $12.00

is the number of statistical segments per strand, L^{-1} is the inverse Langevin function, and $\lambda_i = (1 + \epsilon_i)$ represents the local draw ratio. σ_0 in eq 3 represents the stress in the absence of strain, i.e., that for which $\lambda = 1$. In our approach, a chain strand breaks when it reaches its maximum elongation, i.e., at a local draw ratio $\lambda = n^{1/2}$. In contrast to our previous work, the possibility of chain slippage through entanglements is not considered as our main focus is on the importance of molecular attraction forces. We note also that, once broken, attractive bonds are not being re-formed in our simulations. This is justified by the fact that eq 3 implicitly takes into account strain-induced crystallization effects at high extensions.

Simulation. The simulation of the breaking of the attractive and crystalline bonds is performed with the help of a Monte Carlo lottery which breaks a bond i according to a probability

$$p_i = \nu_i/\nu_{\max} \tag{4}$$

where ν_i is obtained from eq 1 and $\nu_{\max}$ is the rate of breaking of the most strained bond in the array. After each visit of a bond, the "time" t is augmented by $1/[\nu_{\max} n(t)]$, where $n(t)$ is the total number of intact bonds at time t. In addition to those bond breakings, chain strands are also allowed to break when their local draw ratio exceeds its maximum value. After a very small time interval δt has elapsed, the bond and chain breakings are halted and the network of entanglements is elongated along the y-axis by a small constant amount that is determined by the rate of elongation $\dot{\epsilon}$. Subsequently, the network is relaxed to its minimun energy configuration by a series of fast computer algorithms which steadily reduce the net residual force acting on each entanglement point.[5,7,8,13] To save computer time, only displacements along the draw axis are explicitly calculated. Upon reaching mechanical equilbrium, the Monte Carlo process of bond and chain breakings is restarted for another time interval δt until the network fails.

Parameters. The values of the model parameters are as follows.

(i) Flexible-Chain Network. For simplicity, we assume an infinite molecular weight for the chains. A detailed study of the effects of finite chain length can be found in ref 13. The number of statistical segments between entanglements is set arbitrarily at $n = 50$. We note that the latter value corresponds to a maximum draw ratio $\lambda_{\max} = 2^{1/2}\ n^{1/2} = 10$,[17] which is close to the value predicted for amorphous nylon 6,6 with $M_n = 20\,000$.[18] The value of the amorphous chain modulus E_a can be obtained from[14]

$$E_a = 3NkT \tag{5}$$

in which N denotes the density of chain strands between entanglements. Modulus estimates[13,14] based on eq 5 and experimental values[19] obtained from the rubbery shear modulus indicate that E_a for various polymers is of the order of a few MPa. Our simulations are for two different values: $E_a = 1$ MPa and $E_a = 3$ MPa.

(ii) Network of Crystalline and Attractive Bonds. In eq 2, we took $E_c = 10$ GPa. Estimates for E_h can be easily obtained experimentally from the modulus value of the undeformed polymer at low strains. In the present work, E_h is left to vary within the range 0.05−1.8 GPa, which covers the experimental values for most polymers.[20] In eq 1, the actual value of the activation energy, U, for bond breaking is of minor importance as the parameter mainly controls the melting temperature, which is not under study in the present work. Thus, as in ref 16, we choose $U = 35$ kcal/mol. The value of the activation volume β, on the other hand, determines the elongation at break. In order to keep the number of independent variables to a minimum, we elect to make β inversely proportional to E ($=E_h$ or E_c) (see eqs 1 and 2) so that all crystalline and attractive bonds break at same strain $\epsilon_b = 0.1$. As a result, in all our simulations, an increase in the modulus E of a bond also leads a proportional increase in its tensile strength.

(iii) Testing Conditions. We took $T = 300$ K and a strain rate $\dot{\epsilon} = 1$/min.

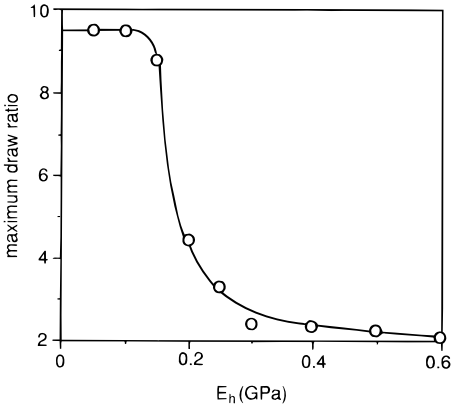

Figure 2. Dependence of the maximum draw ratio on the modulus E_h of the attractive bonds along chains. The figure is for a crystalline volume fraction $V_c = 0$ and a modulus for the amorphous chain network $E_a = 1$ MPa.

3. Results and Discussion

Sections i and ii focus on the dependence of drawability on the moduli E_h and E_a under optimum conditions, i.e., for a crystalline volume fraction $V_c = 0$. Such a situation can be realized experimentally through a fast quenching of the polymer from the melt. Further limitations in drawability due to crystallinity are studied in section iii.

(i) Importance of Modulus E_h (or Strength) of Attractive Bonds. Figure 2 shows our calculated dependence of the maximum draw ratio, i.e., the draw ratio at break, on the modulus E_h of the attractive bonds between chains. The modulus of the amorphous chain network is set at $E_a = 1$ MPa and the results are for optimum drawing conditions, i.e., for a crystalline volume fraction $V_c = 0$. At small $E_h < 0.1$ GPa, all the samples can be easily drawn up to their maximum achievable value $\lambda_{\max} \approx 10$, as determined by the number of statistical segments between entanglements (see section 2). At higher $E_h > 0.1$ GPa, the draw ratio shows a dramatic decrease within a very narrow interval $0.1 < E_h < 0.3$ GPa. The stress−strain curves obtained at each side of that interval are shown in Figures 3a,b. Both curves show the presence of a yield point at ∼10% strain ($\lambda \sim 1.1$), which marks the onset of breaking of the attractive bonds along and between chains (see section 2). Note the much larger yield stress value $\sigma_{\text{yield}} \approx 40$ MPa at $E_h = 0.3$ GPa. These attractive bond breakings usually start at a small defect and, because of local stress concentration effects, they quickly propagate transversally in a direction perpendicular to the draw axis. That process leads to the formation of a very thin region or "neck" entirely made of amorphous chains now free of their attractive intermolecular bonds.

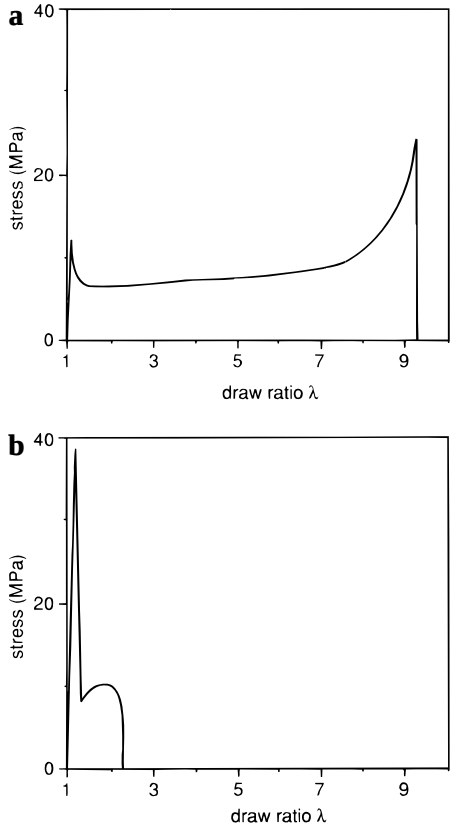

Figure 3. Stress−strain curves at two different E_h values: (a) $E_h = 100$ MPa; (b) $E_h = 300$ MPa. Other parameter values are the same as in Figure 2.

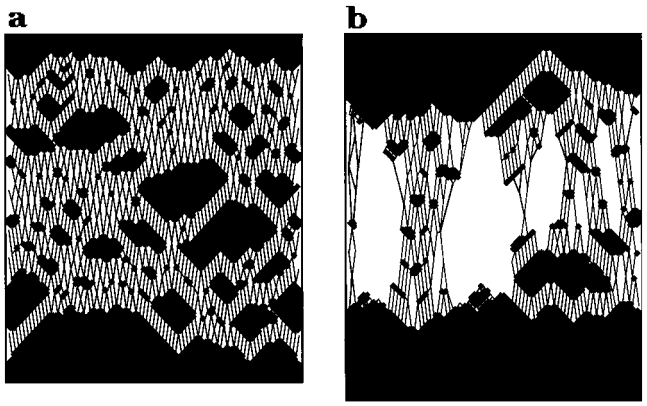

Figure 4. Typical morphologies obtained at $\lambda = 1.6$ for the two cases studied in Figure 3: (a) $E_h = 100$ MPa; (b) $E_h = 300$ MPa.

Since $E_a << E_h$, further deformation of the sample occurs entirely within the neck, leading to a fast increase in the local stress. When the latter reaches the yield stress, the bond breakings resume at the two edges with the undeformed sample, leading to the incorporation of more chain strands into the neck. From these considerations, we easily infer that the poor drawability observed in Figure 3b is due to the fact that σ_{yield} is too large as compared to the highest stress value achievable in the neck for our choice $E_a = 1$ MPa. As a result, the chain strands within the neck rapidly reach maximum extension and break, leading to premature failure of the sample.

Figures 4a,b show details of the morphology of deformation at $\lambda = 1.6$ for the two cases studied in Figures 3a,b. The figures confirm the presence of a neck with a substantial amount of chain breaking at $E_h =$ 0.3 GPa (Figure 4b). Note that, in both cases, the necks are not homogeneous as they contain a large number of small still-undeformed domains. Further investigation reveals that these features are characteristic of high molecular weight polymers. Necks having a more homogeneous structure and sharper boundaries with the undeformed region have been obtained in previous model studies through a decrease in molecular weight and/or entanglement density.[7,13]

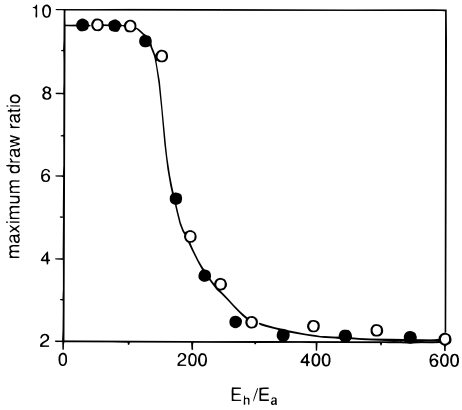

Figure 5. Dependence of the maximum draw ratio on E_h/E_a for two different values of the amorphous chain network E_a. Symbols are as follows: (○) $E_a = 1$ MPa; (●) $E_a = 3$ MPa. The figure is for a crystalline volume fraction $V_c = 0$.

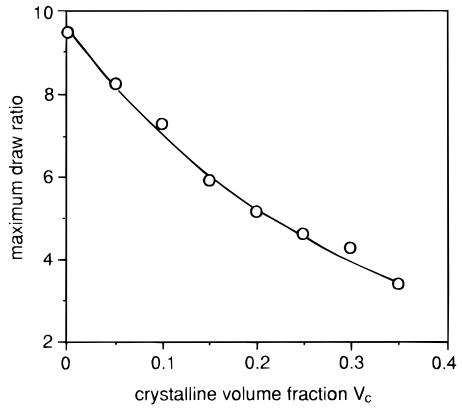

Figure 6. Dependence of maximum draw ratio on crystalline volume fraction V_c. The figure is for a ratio $E_h/E_a = 71$.

(ii) Importance of Modulus E_a of Amorphous Chains. Figure 5 shows the dependence of the maximum draw ratio on E_h/E_a for two different values of E_a ($E_a = 1$: symbol ○ and $E_a = 3$ MPa: symbol ●). Again, we took a crystalline volume fraction $V_c = 0$. The figure clearly reveals that the two sets of data fall on the same master curve. This in turn indicates that the deformation behavior is entirely controlled by the *ratio* E_h/E_a. These findings are of importance as our model results of Figure 5 predict that, in all polymeric materials with $E_h/E_a > \sim 150$, the drawability is limited by the strength of the attractive bonds between chains in the amorphous phase. We note also that, for a given polymer, the ratio E_h/E_a can be varied in two possible ways: (i) through a complexation of the chains with small molecules, leading to a change in the strength of the interactions between chains, and (ii) through a suitable cross-linking of the chains, leading to a higher density of load-bearing chain strands and hence to a larger E_a value.

(iii) Importance of Crystalline Volume Fraction V_c. The effect of crystallinity is studied in Figure 6 for a ratio $E_h/E_a = 71$, at which the drawability for the noncrystalline material is at its maximum achievable

value (see Figure 5). The figure clearly indicates a slow and monotonic decrease in draw ratio with an increase in the crystalline volume fraction, V_c. Our data also indicate that at $V_c > 0.3$, the drawability becomes fully determined by the crystallites and actual values of the E_h/E_a ratio are of secondary importance.

4. Conclusions

We have presented a model study of the factors controlling the drawability of semicrystalline polymers. Our approach focuses on the relative importance of the strength, σ_h, of the attractive bonds between chains in the amorphous phase and of that, σ_a, of the same chains free of attraction forces. We find that drawability reaches its maximum value when the ratio of the two strengths falls below a critical value $\sigma_h/\sigma_a \sim 150$. The maximum draw value itself is controlled by the crystallinity and by the entanglement density in the amorphous phase. At crystalline volume fractions $V_c > 0.3$, the crystallites play a major role in controlling drawability and actual values of the E_h/E_a ratio become of secondary importance.

References and Notes

(1) *Ultra-High Modulus Polymers*; Ciferri, A., Ward, I. M., Eds., Applied Science: London, 1978.
(2) *Strength and Stiffness of Polymers*; Plastic Engineering Series; Zachariades, A. E., Porter, R. S., Eds.; Marcel Dekker: New York, 1983; Vol. 4.
(3) Irvine, P. A.; Smith, P. *Macromolecules* **1986**, *26*, 240.
(4) Postema, A. R.; Smith, P. *Macromolecules* **1990**, *23*, 3296.
(5) Termonia, Y.; Smith, P. *Macromolecules* **1993**, *26*, 3738.
(6) Smith, P.; Matheson, R. R.; Irvine, P. A. *Polym. Commun.* **1984**, *25*, 294.
(7) Termonia, Y.; Smith, P. *Macromolecules* **1987**, *20*, 835.
(8) Termonia, Y.; Smith, P. *Colloid Polym. Sci.* **1992**, *270*, 1085.
(9) Smith, P.; Lemstra, P. J.; Booij, H. C. *J. Polym. Sci., Polym. Phys. Ed.* **1981**, *19*, 877.
(10) Smith, P.; Lemstra, P. J. *J. Mater. Sci.* **1980**, *15*, 505.
(11) Postema, A. R.; Smith, P.; English, A. D. *Polym. Commun.* **1990**, *31*, 444.
(12) Smook, J.; Vos, G. J. H.; Doppert, H. L. *J. Appl. Polym. Sci.* **1990**, *41*, 105.
(13) Termonia, Y.; Smith, P. *Macromolecules* **1988**, *21*, 2184, 3485.
(14) Termonia, Y. *Macromolecules* **1994**, *27*, 7378.
(15) See, e.g., the review in: Kausch, H. H. *Polymer Fracture;* Springer-Verlag: Berlin, 1978; Chapter IV.
(16) Termonia, Y. *Macromolecules* **1994**, *27*, 7378.
(17) The factor $2^{1/2}$ arises because of network considerations on the square lattice; see also ref.13.
(18) Smith, P.; Matheson, R. R.; Irvine, P. A. *Polym. Commun.* **1984**, *25*, 294.
(19) Van Krevelen, D. W. *Properties of Polymers*, 3rd ed.; Elsevier: Amsterdam, 1990; p 383.
(20) Reference 19, p 417.

MA951661X